

Coulomb excitation of a ^{242}Am isomeric target: $E2$ and $E3$ strengths, rotational alignment, and collective enhancement

A. B. Hayes,^{1,*} D. Cline,¹ K. J. Moody,² I. Ragnarsson,³ C. Y. Wu,² J. A. Becker,² M. P. Carpenter,⁴ J. J. Carroll,⁵ D. Gohlke,⁵ J. P. Greene,⁴ A. A. Hecht,^{4,6} R. V. F. Janssens,⁴ S. A. Karamian,⁷ T. Lauritsen,⁴ C. J. Lister,⁴ R. A. Macri,² R. Propri,⁵ D. Seweryniak,⁴ X. Wang,⁴ R. Wheeler,⁵ and S. Zhu⁴

¹*Department of Physics and Astronomy, University of Rochester, Rochester, New York 14627, USA*

²*Lawrence Livermore National Laboratory, Livermore, California 94550, USA*

³*Department of Mathematical Physics, Lund Institute of Technology, SE-221 00 Lund, Sweden*

⁴*Physics Division, Argonne National Laboratory, Argonne, Illinois 60439, USA*

⁵*Department of Physics and Astronomy, Youngstown State University, Youngstown, Ohio 44555, USA*

⁶*Department of Chemical and Nuclear Engineering, University of New Mexico, Albuquerque, New Mexico 87106, USA*

⁷*Joint Institute for Nuclear Research, 141980 Dubna, Moscow, Russia*

(Received 2 August 2010; published 29 October 2010)

A 98% pure $^{242\text{m}}\text{Am}$ ($K = 5^-, t_{1/2} = 141$ years) isomeric target was Coulomb excited with a 170.5-MeV ^{40}Ar beam. The selectivity of Coulomb excitation, coupled with the sensitivity of Gammasphere plus CHICO, was sufficient to identify 46 new states up to spin $18\hbar$ in at least four rotational bands; 11 of these new states lie in the isomer band, 13 in a previously unknown yrast $K^\pi = 6^-$ rotational band, and 13 in a band tentatively identified as the predicted yrast $K^\pi = 5^+$ band. The rotational bands based on the $K^\pi = 5^-$ isomer and the 6^- bandhead were populated by Coulomb excitation with unexpectedly equal cross sections. The γ -ray yields are reproduced by Coulomb excitation calculations using a two-particle plus rotor model (PRM), implying nearly complete $\Delta K = 1$ mixing of the two almost-degenerate rotational bands, but recovering the Alaga rule for the unperturbed states. The degeneracy of the 5^- and 6^- bands allows for precise determination of the mixing interaction strength V , which approaches the strong-mixing limit; this agrees with the 50% attenuation of the Coriolis matrix element assumed in the model calculations. The fractional admixture of the $I_K^\pi = 6_6^-$ state in the nominal 6_5^- isomer band state is measured within the PRM as $45.6_{-1.1}^{+0.3}\%$. The $E2$ and $M1$ strengths coupling the 5^- and 6^- bands are enhanced significantly by the mixing, while $E1$ and $E2$ couplings to other low- K bands are not measurably enhanced. The yields of the 5^+ band are reproduced by an $E3$ strength of ≈ 15 W.u., competitive with the interband $E2$ strength. Alignments of the identified two-particle Nilsson states in ^{242}Am are compared with the single-particle alignments in ^{241}Am .

DOI: [10.1103/PhysRevC.82.044319](https://doi.org/10.1103/PhysRevC.82.044319)

PACS number(s): 21.10.Ky, 23.20.Js, 25.70.De, 27.90.+b

I. INTRODUCTION

Conservation of the angular momentum projection on a symmetry axis of a rotating body is a fundamental property of both classical and quantum mechanical systems. In the nucleus, where this projection is called K , the K -selection rule forbids electromagnetic (EM) transitions of multipole order λ for which $|\Delta K| > \lambda$, giving rise to K isomerism in deformed nuclei. K mixing is a phenomenon often revealed by the fact that K isomers have finite lifetimes, but it has proven difficult to assess the wave functions of mixed- K states quantitatively. There has been some success with various degrees of model dependence [1–8]. The interaction matrix elements giving rise to K mixing are difficult, if not impossible, to deduce from the observed level energy splittings alone.

The initial goal of the present work was to search for low-lying states that could be populated electromagnetically from the $K^\pi = 5^-, t_{1/2} = 141$ years, $^{242\text{m}}\text{Am}$ isomeric state by exploiting K mixing and that would subsequently decay to the $I^\pi = 1^-$ ground state (Fig. 1). There has been much conjecture

in recent years regarding whether various EM processes might be used to depopulate isomeric states [9–11]. Recently, Pálffy *et al.* calculated the probability of EM transitions from nuclear isomeric states following free-electron recombination with an atomic vacancy in $^{242\text{m}}\text{Am}$, among others [12].

Heavy-ion-induced Coulomb excitation is a powerful investigative technique. It favors collective electric quadrupole and octupole excitations in the mass regions of quadrupole-deformed nuclei, so the states coupled to the isomer by strong $E2$ and $E3$ matrix elements are selectively populated. Photoexcitation studies, which have been used to attempt to depopulate isomeric states, are limited by their much lower excitation probabilities and by the requirement that the photon energy be matched to the transition energy. The ability to Coulomb excite numerous states using heavy ions provides an opportunity to study the structure of states strongly coupled to the isomer. In the present work, Gammasphere and the CHICO particle detector [16] provided the necessary resolving power to identify many new γ -ray transitions in the odd-odd ^{242}Am nucleus, despite the low EM transition energies, high internal conversion rates, and high background from the millicurie radioactive target, which presented a challenging experimental problem.

*hayes@pas.rochester.edu

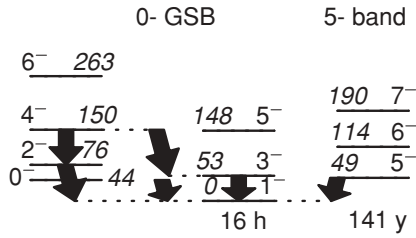


FIG. 1. Previously known low-lying states and transitions in the 0^- band and the 5^- isomer band of ^{242}Am [13–15] and their energies (keV).

II. EXPERIMENT

An $\approx 98\%$ enriched ^{242m}Am isomer sample was separated from contaminants and decay products and electrodeposited onto a 5 mg/cm^2 natural nickel foil at Lawrence Livermore National Laboratory. The isotope was originally prepared at great expense in the 1960s by irradiation of tens of grams of ^{241}Am with epithermal neutrons, followed by chemical processing and two successive isotope separations, resulting in 2 mg of the high-purity product. After measurement of the neutron-induced fission properties, the material was stored in the early 1970s. When the sample was recovered from storage for this experiment, it was found to be distributed over several kilograms of glass, steel, and tantalum. After extensive chemical recovery operations, more than 90% of the original sample was recovered and purified. Particular attention was paid to the removal of other actinide isotopes, which was confirmed by assay. During the present Coulomb excitation experiment, the target contained approximately $2\text{ atom}\%$ ^{241}Am and less than 0.1% ^{243}Am (from incomplete isotope separation), less than 0.04% each of ^{238}Pu and ^{242}Pu , and less than 0.14% ^{242}Cm (from radioactive ingrowth). The equilibrium isomer-to-ground-state ratio in the ^{242}Am sample is 7.7×10^4 . The target was produced by electrodeposition of the nitrate salt from an isopropanol solution directly onto the target backing, with a yield of $>90\%$. A total of $160\ \mu\text{g}$ of material was deposited onto an area 0.65 cm in diameter, for a thickness of $480\ \mu\text{g/cm}^2$. Following the plating process, the foil was heated to 300°C for an hour to fix the ^{242}Am to the nickel backing and then mounted on a target frame with epoxy.

This target was Coulomb excited with a $170.5\text{-MeV } ^{40}\text{Ar}^{9+}$ beam provided by the ATLAS accelerator at Argonne National Laboratory. The de-excitation γ rays were detected by Gammasphere, a 4π , 110-element, Compton-suppressed, high-purity-germanium (HPGe) array, of which 101 detectors were installed [17]. Doppler-shift correction of the de-excitation γ rays was not necessary, as the recoiling ^{242}Am ions were stopped in the target's Ni backing prior to γ decay. In addition, five low-energy photon spectrometers (LEPSSs) were installed in Gammasphere to provide a higher efficiency for transitions with $E \lesssim 300\text{ keV}$ and sufficient resolution to identify K x-ray transitions at 106.5 and 123.7 keV from Am atoms excited by the beam.

The $160\text{-}\mu\text{g}$ target had a calculated activity of $\approx 1.6\text{ mCi}$. To reduce the high rate of random γ -ray coincidences, events were triggered by a coincidence among a backscattered Ar ion detected by CHICO [16], Rochester's parallel-plate

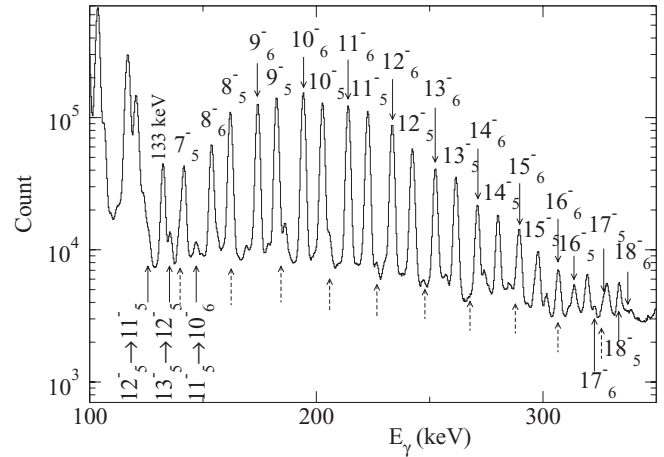


FIG. 2. A partial γ -ray energy spectrum from particle- γ coincidences. Initial and final states are labeled I_K^π . Strong in-band $I \rightarrow I - 2$ transitions are labeled with the initial spin only. Solid (dashed) arrows mark the positions of transitions in ^{242}Am (^{241}Am). Unlabeled strong low-energy peaks are dominated by x rays from the target activity.

avalanche counter (PPAC), and at least one clean photon (not scattered into the BGO Compton suppressors) recorded by a Gammasphere detector or a LEPS. The combined selectivity of CHICO plus Gammasphere produced clean spectra despite count rates of $\sim 500\text{ kHz}$ from x rays in Gammasphere and $\sim 1\text{ MHz}$ in CHICO, owing to the natural α activity of the target. An $\approx 30\text{-ns}$ time gate was placed on the germanium time signal relative to the particle time signal, improving the peak-to-background ratio by a factor of 5 (Fig. 2). During 106 h of beam at $\sim 0.3\text{ particle nA}$, approximately 3×10^7 particle- γ ($p\text{-}\gamma$) events satisfying the time requirement were recorded.

The high-resolution γ -ray energy spectrum measured by the LEPS detectors was used to ensure that measured γ -ray yields were not contaminated by doublets in the Ge spectrum for this high-level-density, odd-odd nucleus. The Coulomb excitation yields of the low-lying states in ^{241}Am [18] were used to measure the $\approx 2\%$ ^{241}Am contaminant in the target, confirming the target assay. No other γ rays from contaminants were observed in the data.

The relative γ -ray efficiency was measured using ^{152}Eu , ^{243}Am , ^{182}Ta , and ^{56}Co radioactive sources. The absolute efficiency was determined using the online $p\text{-}\gamma$ data, as dead time and pileup events from the millicurie target activity effectively reduced the absolute efficiency of Gammasphere. Coulomb excitation calculations for the ^{40}Ar beam, based on known lifetimes and branching ratios of the low-lying ^{40}Ar states, were compared to the measured yields to derive the absolute efficiency ϵ_{abs} of the $1461\text{-keV}, ^{40}\text{Ar } 2_1^+ \rightarrow 0_1^+$ transition using the relation

$$\epsilon_{\text{abs}} \frac{\sigma_{1461}}{\sigma_R} = \frac{Y_{1461;\text{Am}}}{Y_{\text{Am}}}. \quad (1)$$

Here, σ_{1461} is the calculated Coulomb excitation cross section, σ_R is the Rutherford cross section, and $Y_{1461;\text{Am}}$ and Y_{Am} are the $1461\text{-keV } \gamma$ -ray yield in coincidence with a ^{242}Am transition and the ungated yield of the same ^{242}Am transition,

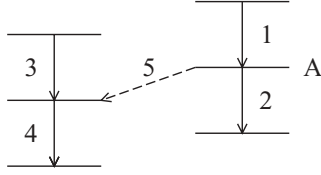


FIG. 4. A hypothetical level scheme used to illustrate branching ratio measurements for level A. Arrow 5 represents an unobserved highly converted transition.

As illustrated schematically in Fig. 4, gating on coincident γ -ray transitions branching ratios can be obtained using the relations

$$\frac{\Gamma_5}{\Gamma_T} = \frac{Y_{4;1}Y_3}{Y_1Y_{4;3}}, \quad (2)$$

where Y_j is the γ -ray intensity of transition j in the p - γ spectrum, and $Y_{j;k}$ is the γ -ray intensity of transition j with a gate on transition k in the p - γ - γ matrix. The internal conversion and efficiency corrections cancel identically. Similarly,

$$\frac{\Gamma_2}{\Gamma_T} = \frac{Y_{2;1}(1 + \alpha_2)}{\epsilon_2 Y_1}, \quad (3)$$

where α_2 and ϵ_2 are the internal conversion coefficient and the absolute γ -ray detection efficiency of transition 2, respectively.

In most cases there is at least one alternate decay path between the initial state ‘‘A’’ and the final state of transition ‘‘5’’ whose width is to be measured. If a sufficient number of gating transitions above and below transition 5 are available, repeated subtractions can be used to separate the other decay paths between the initial and the final states from the desired branch A. Nine states had sufficient data to untangle the fractional widths and ensure that they sum to 1. With the exception of the $I^\pi = 13^-$ state in the 6^- band, the sum was within 1σ of unity in every case, thereby validating the absolute efficiency determination. The measured total ($\gamma + e^-$) branching ratios are presented in Figs. 5 and 6.

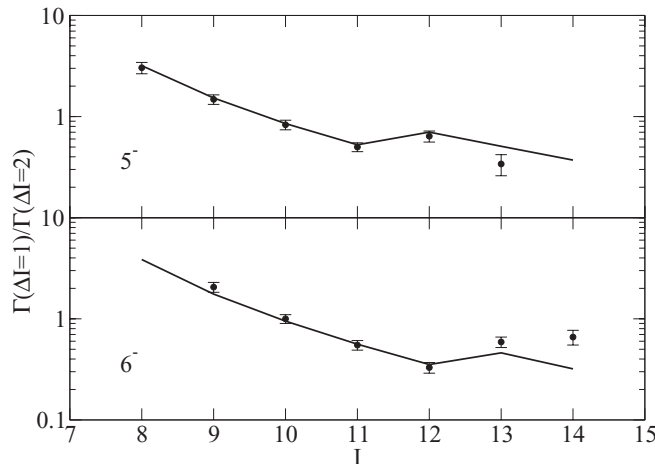


FIG. 5. Measured (points) intraband branching ratios $\Gamma_{\Delta I=1}/\Gamma_{\Delta I=2}$ including electron conversion. Calculated values (lines) are from calculations using the tuned PRM.

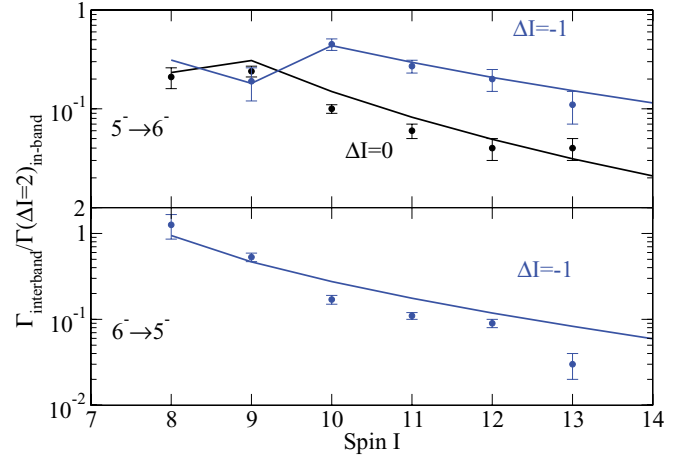


FIG. 6. (Color online) Measured (symbols) and calculated (lines) interband branching ratios $\Gamma_{\text{interband}}/\Gamma_{\text{inband}}$ including electron conversion. Calculated branching ratios are from calculations using the tuned PRM.

B. The γ -ray yields

Coulomb excitation γ -ray yields were measured wherever possible using the p - γ coincidence spectrum, as branching ratios necessary to correct gated p - γ^2 , p - γ^3 data are not known to a high precision. The measured and calculated yields quoted here were normalized to the 203-keV, $I_K^\pi = 10_5^- \rightarrow 8_5^-$, $E2$ yield (Fig. 3).

C. The 5^- and 6^- bands

The 5^- and 6^- bands were constructed (Fig. 3) by gating in the p - γ^2 matrix, starting from the known $7_5^- \rightarrow 5_5^-$ transition and deducing the spins of the newly established levels from the $E2$ transitions. In total, 24 new states were added to the known 5^- and the newly identified 6^- bands [13–15]. The γ -ray energies of the $\Delta I = 2$ in-band transitions have errors of <0.5 keV, and the resulting level energies (calculated by summing the transition energies) have errors of ≤ 2 keV.

The preceding gating procedure determined the ordering of the states, but the absolute energies for the 6^- band members could be determined only within the limits set by the bounds of the adjacent 5^- states. Fortunately, the highly converted branches between the 5^- and the 6^- bands exhibited discontinuities in intensity as the transition energies crossed the 125-keV Am K edge between the $10_5^- \rightarrow 9_6^-$ (133-keV) and the $9_5^- \rightarrow 8_6^-$ (119-keV) decays (Fig. 6). A similar effect was observed between the $9_5^- \rightarrow 9_6^-$ and the $8_5^- \rightarrow 8_6^-$ transitions, owing to the 18.5- to 24-keV L edges. The observation of the K and L edges narrowed the bounds in which to search for the energy of the 6^- bandhead.

Searching within these limits, three of the $\Delta I = -1$ interband γ rays were resolved by gating in the p - γ^2 matrix, while triple- γ coincidence data were used to tentatively identify the 90-keV, $\Delta I = -1$ transition. The energies of the $I^\pi = 6^-$ and 7^- states (100 and 172 keV, respectively) in the 6^- band were then found to agree with previously observed, but unidentified, peaks (99 and 171 keV) in $^{243}\text{Am}(d,t)$ ^{242}Am

spectrograph data [14]. The transfer peaks had strengths consistent with the present identification. In all, 15 $\Delta I = -1$ transitions were identified in the 5^- and 6^- bands (Fig. 3). A number of γ rays with energies of less than 120 keV lie under the strong x-ray background and could not be resolved. The energy of the $I^\pi = 6^-$ state in the 6^- band was thus found to be 100.1(7) keV. The 5^- and 6^- bands were assigned the structures $\pi_{\frac{5}{2}^-}[523](h_{9/2}) \otimes \nu_{\frac{5}{2}^+}[622](i_{11/2})$ and $\pi_{\frac{5}{2}^-}[523](h_{9/2}) \otimes \nu_{\frac{7}{2}^+}[624](g_{9/2})$, respectively, by Salicio *et al.* [15].

D. The $K^\pi = (5^+)$ A and B bands

The tentative $K^\pi = (5^+)$ signatures have in-band $E2$ γ -ray energies within about 1 keV of those in the 5^- band. This (5^+) sequence was resolved using a number of gates in $p\text{-}\gamma^2$ and $p\text{-}\gamma^3$ data sets that clearly distinguished the 182.0-, 202.2-, 222.0-, 241.1-, and 261.2-keV transitions from their doublets in the 5^- band (see, e.g., Figs. 7 and 8).

The $\sim 10^{-2}$ strength of the tentative (5^+) band $E2$ yields normalized to the $10_5^- \rightarrow 8_5^-$ transition implies a close connection with the 5^- band. The strong 132.8-keV decay (Figs. 2 and 3) does not come into coincidence with the $E2$ transitions in the 5^- or 6^- bands, so it most likely corresponds to a decay back to the 5^- isomer state. It cannot be strictly ruled out that this is a feeding transition to the ground-state band (GSB), which would indicate Coulomb de-excitation of the isomer to the ground state. This is, however, less likely if the $K^\pi = 5^+$ assignment is correct, as the decay to the $K^\pi = 0^-$ GSB would then be 4 times K forbidden.

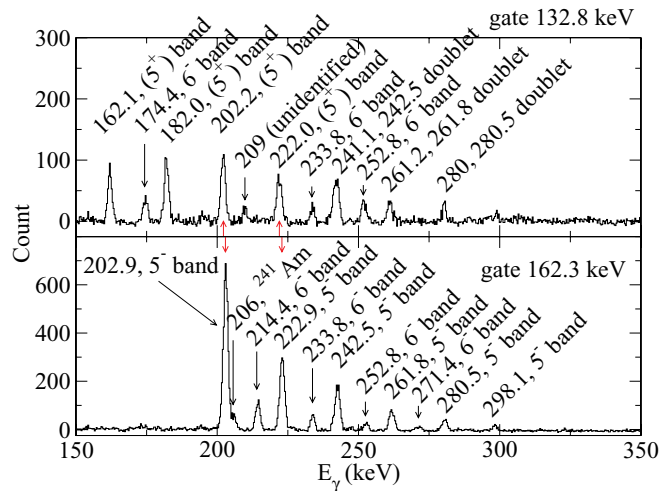


FIG. 7. (Color online) Resultant coincidence spectra after gates in the $\gamma\text{-}\gamma$ matrix. The gate at 162.3 keV (bottom) is coincident predominantly with transitions in the 5^- and 6^- bands, with $\sim 1\%$ doublets from (5^+) band transitions. The gate at 132.8 keV (top) resolves two of the (5^+) band transitions: 202.2 and 222.0 keV. The doublets and 5^- , 6^- band transitions appear owing to the two ≈ 133 -keV transitions in the 5^- and 6^- bands. Red arrows mark the fitted peak energies of two doublets that can be resolved using only these two gates. A number of such gates in the $p\text{-}\gamma^2$, $p\text{-}\gamma^3$ data were used to resolve the (5^+) band transitions. See text for details.

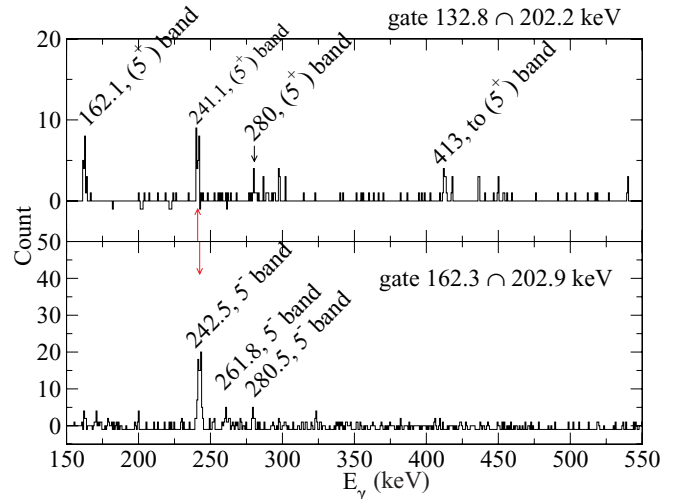


FIG. 8. (Color online) Two pairs of coincidence gates in the $p\text{-}\gamma^3$ data. The 162.3 \cap 202.9-keV gate (bottom) selects predominantly the transitions in the 5^- , 6^- bands and shows no indication of a transition at 413 keV. The 132.8 \cap 202.2-keV gate (top) indicates that the 413-keV transition feeds the (5^+) band above the 202.2-keV intraband transition.

The level energies of the even-spin signatures were established tentatively by using the proposed $\Delta I = 0, 1$ decays from bands A and B. This results in excitation energies for the (5^+) band's even- I states within 3.5 keV of the values that would be obtained assuming no signature splitting. No linking transitions between the signatures were observed. The total intensity of the 132.8-keV γ ray was measured as 53(10)% using the same normalization, indicating the decay of a bandhead preceding by an $E1$ transition, which would have an internal conversion coefficient of 0.27, compared to $\alpha_{132.8\text{keV}}^{E2} = 5.0$, $\alpha_{132.8\text{keV}}^{M1} = 13.1$, $\alpha_{132.8\text{keV}}^{M2} = 71.8$, etc. [27]. Any multipolarity other than $E1$ would indicate stronger Coulomb excitation of the 5^+ band than of the 5^- band, in conflict with the $\sim 1\%$ observed strength of the $K^\pi = (5^+)$ intraband transitions.

The tentative $K^\pi = (5^+)$ assignment is reached through the limits placed on the spin ($4 \leq I \leq 6$) and parity by the $E1$ assignment and by the most likely final state being the 5^- isomer. A previous calculation [15] predicted a $K^\pi = 5^+$ $\pi_{\frac{5}{2}^+}[642](i_{13/2}) \otimes \nu_{\frac{5}{2}^+}[622](i_{11/2})$ level at 193(60) keV, compared to the present tentative placement at 180 keV.

If the spins of the (5^+) signatures were assigned such that the 142.0-keV transitions were from an $I = 7^+$ state to the tentative $I = 5^+$ bandhead, the alignment would be nearly identical to that of the 5^- isomer band (Sec. V G), which is $\approx 1\hbar$ less than the alignment of the $\pi_{\frac{5}{2}^+}[642](i_{13/2})$ orbital in ^{241}Am [18,28]. The alignments of the $\pi_{\frac{5}{2}^+}[642](i_{13/2})$ and $\nu_{\frac{5}{2}^+}[622](i_{11/2})$ orbitals should be additive, which casts doubt either on the $\pi_{\frac{5}{2}^+}[642](i_{13/2}) \otimes \nu_{\frac{5}{2}^+}[622](i_{11/2})$ identification or on the 142.0-keV γ ray being assigned to an initial $I = 7$ state. The alignment of the observed band has the expected additional $\approx 1\hbar$ alignment compared to the $\pi_{\frac{5}{2}^+}[642]$ states

TABLE I. Observed multiplets and selected predicted multiplets in ^{242}Am . Nilsson states $\Omega[Nn_z\Lambda]$ are given as they were assigned in Refs. [14] and [15]. All assignments listed can be coupled to the 5^- , 6^- states by at most a one-body operator. Excitation energies from the present work were measured assuming a 5^- isomer energy of 48.6 keV from previous work [13].

Configuration		Bandhead energy (keV)				Rotational parameter (keV)				
π	ν	K^π	E_{theor}^a	E_{theor}^b	E_{meas}^a	E_{meas}^b	A_{theor}^a	$A_{\text{theor}}^{b,c}$	A_{meas}^a	A_{meas}^b
$\frac{5}{2}^-$	[523]($h_{9/2}$)	$\frac{5}{2}^+$ [622]($i_{11/2}$)	0 ⁻	0	0.0		5.1(4)	5.1	5.28(11)	
		5 ⁻	112(40)	26	48.6		5.1(4)	5.1	5.44(11) ^d	5.20(3)
$\frac{5}{2}^-$	[523]($h_{9/2}$)	$\frac{7}{2}^+$ [624]($g_{9/2}$)	6 ⁻	126(20)	84	100.4	5.3(3)	5.3		5.00(2)
			1 ⁻	288(53)	62	275.3	5.3(3)	5.2	5.7(1)	
$\frac{5}{2}^-$	[523]($h_{9/2}$)	$\frac{1}{2}^+$ [631]($d_{5/2}$)	3 ⁻	169(37)	203	244.4	5.6(2)	5.1	5.57(10)	
			2 ⁻	218(42)	202	292.8	5.6(2)	5.4	5.80(11)	
$\frac{3}{2}^-$	[521]($f_{7/2}$)	$\frac{5}{2}^+$ [622]($i_{11/2}$)	4 ⁻	400(100)	168		5.4(3)	5.2		
			1 ⁻	563(110)	152	400.5	5.4(3)	5.2	5.4(3)	
$\frac{5}{2}^+$	[642]($i_{13/2}$)	$\frac{5}{2}^+$ [622]($i_{11/2}$)	5 ⁺	193(60)	445	(180.4)	3.5(3)	4.6		5.26(2)
			0 ⁺	211(63)	421	230.5	3.5(3)	4.6	4.1(1)	
$\frac{5}{2}^+$	[642]($i_{13/2}$)	$\frac{7}{2}^+$ [624]($g_{9/2}$)	1 ⁺		482			4.7		
			6 ⁺		508			4.7		
$\frac{7}{2}^+$	[633]($i_{13/2}$)	$\frac{5}{2}^+$ [622]($i_{11/2}$)	6 ⁺		672	(514) ^e		5.5		(5.3)
			1 ⁺		636			5.3		

^aFrom Refs. [14] and [15].

^bFrom the present work.

^cValues after tuning of the PRM variable moment-of-inertia parameters so that the 5^- , 6^- bands' calculated moments fit those of the observed states.

^dFor observed states $5 \leq I \leq 7$.

^eThe energy of the unobserved bandhead is extrapolated from the observed states.

in ^{241}Am if the 142.0-keV transition is assigned to an initial $I = 9$ state.

The particle-rotor model (PRM) calculations discussed hereafter predict only one 5^+ state ($\pi \frac{5}{2}^+$ [642] \otimes $\nu \frac{5}{2}^+$ [622] at 445 keV; Table I) within 1.3 MeV of the ground state. This predicted level can couple electromagnetically to the 5^- isomer initial state ($\pi \frac{5}{2}^-$ [623] \otimes $\nu \frac{5}{2}^+$ [622]) by a one-particle operator. Coulomb excitation calculations reproduce the observed 10^{-2} level (5^+) band γ -decay yields using $B(E3)$ values of ≤ 15 W.u. coupling the 5^- and 6^- bands to the (5^+) band, consistent with a one-particle operator, as discussed here.

Choosing to keep the $\pi \frac{5}{2}^+$ [642]($i_{13/2}$) \otimes $\nu \frac{5}{2}^+$ [622]($i_{11/2}$) $K^\pi = 5^+$ assignment, the spins of the floating (5^+) signatures were assigned to give an alignment consistent with the proposed Nilsson states (Sec. V G). In that case, the unobserved $8^+ \rightarrow 6^+$ (≈ 122 -keV) and $7^+ \rightarrow 5^+$ (≈ 102 -keV) transitions would be completely obscured by the x-ray background, consistent with their nonobservation in the p- γ spectra. Considering the predicted energy of the $I_K^\pi = (5_5^+)$ state [15], and the lack of other predicted states nearby that would couple to the isomer band by a one-particle operator consistent with the observed Coulomb excitation strength, these tentative orbital and spin assignments appear to be the best choice available, but the $K^\pi = 5^+$ assignment remains tentative.

A number of the γ transitions feeding into the 5^+ band were tentatively identified as originating from two signatures, A and B, in Fig. 3 with a normalized intensity of $< 1\%$. Assuming

that the pairs of transitions from each state in the A and B bands are of the $\Delta I = 0, -1$ type, the approximately equal intensities of the two branches from each level suggest a small $E2$ component and a predominant $E1$ or $M1$ multipolarity. The final states of these decays were established as the states of the tentative 5^+ band, based on the observed coincidences

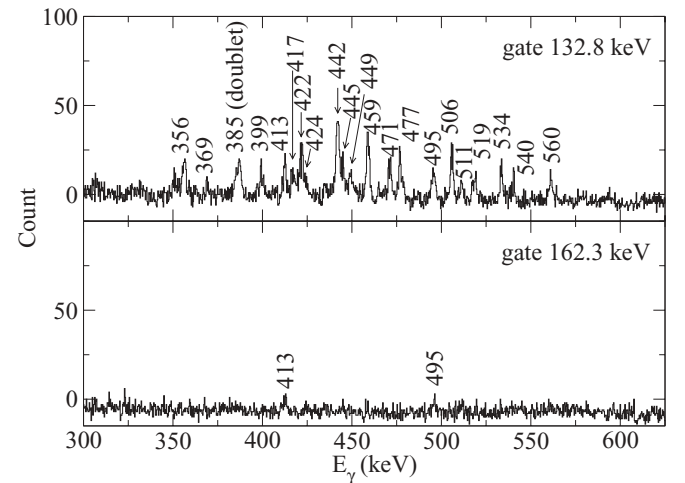


FIG. 9. Two coincidence spectra from the p- γ data gated on the 132.8-keV transition, tentatively assigned as $5_{K=5}^+ \rightarrow 5_{\text{isomer}}^-$, and the 162.8-keV line in the (5^+) band suggesting that the 400- to 600-keV γ rays feed into the tentative $K^\pi = (5^+)$ band, which decays via the 132.8-keV transition.

with transitions in the 5^+ band and the 132.8-keV γ ray (Fig. 9). Those transitions that are in coincidence with the 132.8-keV transition, but not with the transitions assigned to the (5^+) band, were tentatively placed as feeding the bottom of the (5^+) band, where the implied initial state resulted in a smooth moment of inertia. While the assignment of transitions to signatures A and B in the level scheme in Fig. 3 is tentative, this scenario seems more likely than assuming that many more bands (including those of the unidentified transitions in Table II) feed into the 132.8-keV transition and lie within the few units of K reachable from the (5^+) band by the present Coulomb excitation. No intraband transitions could be found in signatures A and B. This is consistent with the expected $\sim 10^{-4}$ strengths for the intraband $E2$ transitions relative to the interband ones assuming a single-particle strength for the ≈ 400 - to 600-keV interband transitions. The greater or equal strength of the lower-energy decay in each de-excitation pair suggests a significant $E1$ or $M1$ branch and $\Delta K = \pm 1$, while the higher intensities of the interband than of the intraband indicate that a one-particle transition is most likely. The PRM calculations (Sec. IV A) predict only two positive-parity bands with $\Delta K = \pm 1$ and with a one-particle EM operator coupling to the proposed $\pi \frac{5}{2}^+ [642] \otimes \nu \frac{5}{2}^+ [622]$ configuration of the 5^+ band. These are two $K^\pi = 6^+$ bands at ≈ 500 and ≈ 670 keV with predominant Nilsson configurations $\pi \frac{5}{2}^+ [642] \otimes \nu \frac{7}{2}^+ [624]$ and $\pi \frac{7}{2}^+ [633] \otimes \nu \frac{5}{2}^+ [622]$, respectively. The lower-energy state seems less likely, as it has (i) a predicted strong mixing with lower K values, with the loss of predominant $K^\pi = 6^+$ character, by $I = 12$ and (ii) a rapidly changing moment of inertia from the mixing, unlike the observed feeding band. The moment of inertia predicted by the PRM for the state of this Nilsson parentage is within 8% of the observed value. The presumed $I_K^\pi = 6_6^+$ bandhead was not observed, possibly owing to the dominant interband cascade and weak intraband decay (below the observational limit). The approximate energy of the 6^+ state, assuming that the band is $K = 6$, is extrapolated using the rotor model and reported in Table I.

E. Search for $0 \leq K \leq 3$ bands

The p - γ spectrum and the p - γ^2 matrix were searched for transitions in the known GSB (Fig. 1), as well as possible extensions of the GSB above $I_K^\pi = 6_0^-$ (based on extrapolations from the known $I \leq 6\hbar$ states [14,15]). No candidates were found. The known in-band GSB transitions would be highly converted and buried under the strong x-ray peaks (Fig. 2), making their observation challenging, if not impossible. The estimated upper bounds of observation in the p - γ^2 matrix place a limit on the γ -decay yield of unobserved GSB states above $I = 6\hbar$ at $\sim 1\%$ relative to the 5^- band yields. No indication could be found that higher order $\Delta K \geq 3$ mixing results in an enhanced $E2$ excitation of the unobserved $I^\pi = 3^-$ GSB state that lies only 4 keV above the $K^\pi = 5^-$ isomer.

There was no sign of the other known or predicted $0 \leq K \leq 3$ bands (Table I and Fig. 12). Preliminary work on this data set tentatively identified the γ rays feeding into the 5^+ band as transitions from the extension of a known 3^- band into the 5^-

TABLE II. Unidentified γ rays. All transitions listed here are tentatively determined to be direct or indirect γ decays feeding the tentative $K^\pi = (5^+)$ band by coincidence with the 132.8-keV, $K^\pi = (5^+) \rightarrow 5^-$ transition. Approximate intensities are given relative to the $10_5^- \rightarrow 8_5^-$ transition assuming that the entire cascades below them feed into the $K^\pi = (5^+) \rightarrow 5^-$ transition.

E_γ (keV)	$I_\gamma 10^{-3}$
209.9	3.7(5)
417.1	3.8(6)
442.0	10.3(11)
449.3	3.4(5)
459.0	8.5(9)
477.1	5.7(8)
505.8	6.3(8)
533.7	5.3(7)
653.5	2.8(7)
662.9	3.5(6)

isomer band [29], because the energies of the in-band $K^\pi = 5^+$ $E2$ lines are nearly identical to those of the 5^- band. Correct identification of the doublets and the present placement of the 132.8-keV $5_{K=5}^+ \rightarrow 5_{\text{isom}}^-$ transition are not consistent with the previous tentative 3^- band assignment. Transitions shown in Fig. 3 feeding into the 5^+ band have been separated into tentative bands, where their energies are consistent with an assignment to individual rotational sequences. While the lack of observed in-band transitions prevents a definite assignment, none appear to be consistent in spin and energy with the $K^\pi = 3^-$ band. The known 132.565-keV $3_2^+ \rightarrow 3_3^-$ transition [15] was ruled out as corresponding to the present 132.8-keV γ ray by the upper limits on the intensities of the unobserved lines that would accompany the 132.565-keV transition. These upper limits were found to be 5—30 times smaller than would be the case if the present 132.8-keV γ ray were the known $3_2^+ \rightarrow 3_3^-$ transition.

Similarities between the energies of the observed transitions into the $K^\pi = 5^+$ band and those from known $K^\pi = \frac{3}{2}^-$ band states in ^{241}Am were found to be accidental. In all but one case, the energies differ by ≥ 2 keV from those of ^{241}Am [18]. Furthermore, the strongest transitions in the $\approx 2\%$ ^{241}Am target contaminant were observed at the $\approx 3\%$ level. Previous “unsafe” Coulomb excitation of ^{241}Am [18,28] showed that the $K^\pi = \frac{3}{2}^-$ band should be populated at the 10^{-3} level relative to the GSB, so the presently observed $\lesssim 1\%$ Coulomb excitation yield of these transitions is more than 3 orders of magnitude too high to be attributed to the ^{241}Am target contaminant.

IV. COULOMB EXCITATION ANALYSIS AND MODEL CALCULATIONS

A. Particle-rotor model

A PRM appropriate for the description of odd-odd collective nuclei [30], based on an earlier one-particle plus rotor model [31], was used to predict the structures and transition strengths of low-lying states in ^{242}Am . The model parameters

were tuned such that semiclassical coupled-channels Coulomb excitation calculations with GOSIA 2008 [32,33] using the PRM's $E2$ and $M1$ matrix elements reproduce the observed γ -ray yields. These calculations assumed a modified oscillator potential to calculate Nilsson states. The latter were obtained separately for the unpaired proton and neutron, and a set of basis states near the Fermi level was selected. The oscillator parameters for the protons and neutrons were taken from Rozmej *et al.* [34], as cited in Ref. [35]: $\kappa_\pi = 0.058$, $\mu_\pi = 0.63$, $\kappa_\nu = 0.0526$, $\mu_\nu = 0.457$. The initial values of the deformation parameters were taken from the calculations of Möller and Nix [36], which give $\epsilon_2 = 0.21$ and $\epsilon_4 = -0.05$. The quadrupole deformation was subsequently adjusted to $\epsilon_2 = +0.2344$, so that the microscopic calculation of the intrinsic quadrupole moment reproduced the value $Q_0 = 11.73$ b interpolated from neighboring nuclei [37]. No triaxiality was assumed, and the value of ϵ_6 was set to 0.

Following the calculation of these states, the pairing terms were computed using the BCS approximation, except in the case of the neutron Fermi level, which was tuned to adjust the mixing in the nearly degenerate 5^- and 6^- bands until agreement with the Coulomb excitation yields was achieved. The proton Fermi level was calculated using pairing strength parameters adjusted to 95% of the values fit to even-even nuclei [38], giving $G_{N0} = 18.2$ and $G_{N1} = 7.0$ so that $GA = G_{N0} + G_{N1} \frac{N-Z}{A} = 20.1$. The pairing factors were taken to the first power ($\eta = 1$) in all cases, while the Coriolis attenuation factor was assumed to be $\xi = 0.5$, a typical value for the actinide region [1,39–41].

The variable moment-of-inertia parameters were adjusted to reproduce the moments of inertia of the observed states of the 5^- and 6^- bands only, which were the only states identified confidently. These parameters are the first-order inertia term A_0 and the second-order (stiffness) term A_1 . From the moment-of-inertia parameters and the basis states, single-particle energies and $E2$ and $M1$ matrix elements were calculated using the PRM Hamiltonian and even multipole deformations. The value of g_s^{eff} was set to $0.7g_s^{\text{free}}$, a typical estimate [39], which reproduced the known magnetic moments well (Sec. IV B). The residual V_{pn} proton-neutron interaction was not included in the calculations. Further descriptions of the relevant parameters are given in Refs. [30] and [31] and references therein.

B. The 5^- , 6^- bands

The nearly equal population of the 5^- and 6^- bands implies the presence of strong mixing between these two structures. This is confirmed by a Coulomb excitation calculation using GOSIA assuming 1-W.u. $E2$ and $M1$ matrix elements coupling the 5^- and 6^- bands (assuming that $K^\pi = 5^-, 6^-$ mixing is negligible). The intrinsic quadrupole moment $\sqrt{\frac{5}{16\pi}}eQ_0$ was fixed at 3.7 eb, consistent with values from neighboring nuclei [37], and the $g_K - g_R$ values were taken from the PRM calculations (see the following). The Coulomb excitation yields of the 6^- band are not reproduced assuming unmixed bands using the Alaga rule (Fig. 10). In fact, $E2$ reduced transition probabilities as high as 340 W.u. coupling the 5^- and 6^- bands (at least 1 order of magnitude too large for

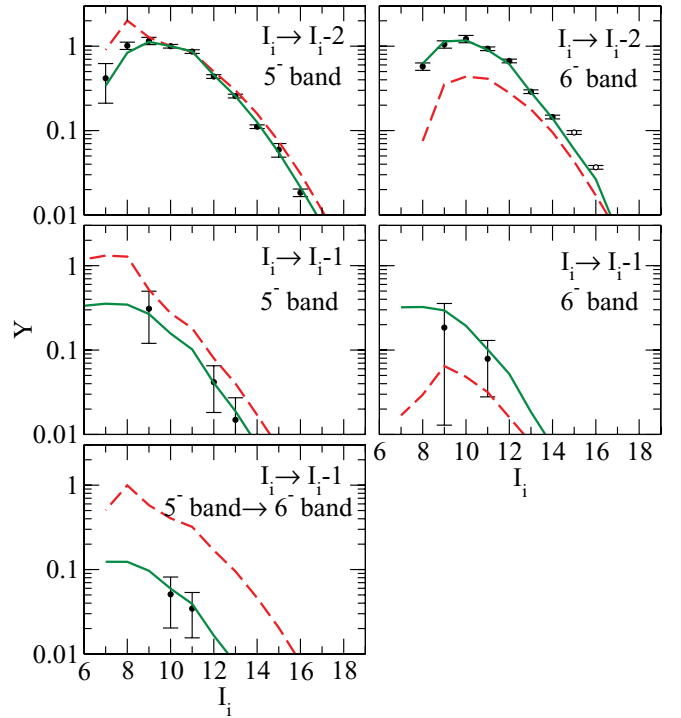


FIG. 10. (Color online) Measured (symbols) and calculated (lines) γ -ray yields Y in the 5^- and 6^- bands normalized to the $I^\pi = 10^- \rightarrow 8^-$ transition in the 5^- band. Solid (green) lines are from the PRM fit; dashed (red) lines were calculated using the Alaga rule with $\langle K = 6 | E2 | K = 5 \rangle = 1$ W.u., neglecting $K = 5, 6$ mixing. Yields for the interband transitions are from a gated γ - γ matrix. The 6^- band transitions whose yields are represented by open symbols are believed to be members of doublets and were not included in the fit (see text).

a single-particle transition) are necessary to obtain rough agreement with the data. These observations indicate that mixing between the two nearly degenerate bands is strong and that an accurate analysis requires consideration of the mixing. The Coulomb excitation calculations show that the populations of high-spin states are improved only slightly, suggesting that mixing is most important at low spin. PRM calculations were then performed to reproduce the experimental γ -ray yields of the 5^- and 6^- bands and to deduce the mixing fraction $\beta^2(I)$ between the bands using the present data.

The Coulomb excitation γ -ray yields were reproduced using GOSIA by adjusting the neutron Fermi level from the PRM calculated value of 53.321 to 53.374 MeV. This resulted in mixing between the 5^- and the 6^- bands that was sufficient to reproduce the observed populations of both bands. Because the 5^- and 6^- bands share a common proton orbital (Table I), the yields were not sensitive to the proton Fermi level λ_π , and no adjustment was made to the value of λ_π given by the BCS calculations.

In the limit of strong mixing indicated by the comparably strong 5^- and 6^- band yields and predicted by the fit of the neutron Fermi level, the interaction between these two bands can be treated as in a simple two-state mixing formalism, neglecting small admixtures of other K values in the wave function. In the PRM calculations, all admixtures other than

$K = 5, 6$ in the wave function sum to $\approx 0.5\%$ at $I = 6$ and 5% at $I = 18$. The interband matrix elements for two-state mixing take the form

$$\begin{aligned} & \langle I_f^{VI} \| E2 \| I_i^V \rangle \\ &= \sqrt{2I_i^V + 1} \left[\sqrt{\frac{5}{16\pi}} e Q_0 (\alpha_f \beta_i \langle I_i^V 6 2 0 | I_f^{VI} 6 \rangle \right. \\ & \quad - \alpha_i \beta_f \langle I_i^V 5 2 0 | I_f^{VI} 5 \rangle) + \langle 6 | E2 | 5 \rangle \\ & \quad \left. \times (\beta_i \beta_f \langle I_i^V 6 2^{-1} | I_f^{VI} 5 \rangle + \alpha_i \alpha_f \langle I_i^V 5 2 1 | I_f^{VI} 6 \rangle) \right], \end{aligned} \quad (4)$$

$$\begin{aligned} \langle I_f^{VI} M1 \| I_i^V \rangle &= \sqrt{2I_i^V + 1} \left[\sqrt{\frac{3}{4\pi}} \mu_N (6\alpha_f \beta_i (g_K - g_R)_6 \right. \\ & \quad \times \langle I_i^V 6 1 0 | I_f^{VI} 6 \rangle - 5\alpha_i \beta_f (g_K - g_R)_5 \\ & \quad \times \langle I_i^V 5 1 0 | I_f^{VI} 5 \rangle) + \langle 6 | M1 | 5 \rangle \\ & \quad \times (\alpha_i \alpha_f \langle I_i^V 5 1 1 | I_f^{VI} 6 \rangle \\ & \quad \left. + \beta_i \beta_f \langle I_i^V 6 1^{-1} | I_f^{VI} 5 \rangle) \right], \end{aligned} \quad (5)$$

with the wave functions defined by

$$\begin{aligned} \| I^V \rangle &= \alpha \| I, K = 5 \rangle + \beta \| I, K = 6 \rangle, \\ \| I^{VI} \rangle &= -\beta \| I, K = 5 \rangle + \alpha \| I, K = 6 \rangle, \end{aligned} \quad (6)$$

where the labels V and VI indicate the observed mixed $K^\pi = 5^-$ and 6^- states, respectively, and α and β are the mixing amplitudes in the wave functions of Eqs. (6). (Mixing fractions quoted here refer to the quantity β^2 .) The intrinsic matrix elements $\langle 6 | E2 | 5 \rangle$ and $\langle 6 | M1 | 5 \rangle$ and the $g_K - g_R$ values refer to the pure $K = 5$ and 6 components in the wave functions. Collective enhancement can be seen mathematically as arising from the interference between the terms related to single-particle transitions ($\langle 6 | E2 | 5 \rangle$ and $\langle 6 | M1 | 5 \rangle$) and the usual moments for in-band transitions (Q_0 and $g_K - g_R$). The forms of the intraband matrix elements are similar. The reduced matrix elements from the model do not follow the Alaga rule, but the Alaga rule is recovered in terms of the hypothetical unperturbed states.

The Coulomb excitation γ -ray yields were reproduced using the matrix elements predicted by the tuned PRM calculations in GOSIA, giving $\chi_{\text{red}}^2 = 0.88$ for 25 data points and three adjustable parameters, A_0 , A_1 , and λ_v (Fig. 10). The Coulomb excitation data are consistent with the value assumed for the quadrupole moment. [The γ -ray yields for $I > 14$ in the 6^- band (Fig. 10) are 8σ too high to be explained by Coulomb excitation, which is expected to decrease approximately exponentially with spin [42]. These large yields are believed to be the result of the presence of unidentified doublets and were left out of the fit.]

While it is usually not possible to determine the signs of magnetic parameters in Coulomb excitation, reproduction of the $E2$ and $M1$ γ -ray intensities in the present data is sensitive to strong interference terms in the reduced matrix elements [e.g., Eq. (5)]. With the choice to fix the $g_K - g_R$ values calculated by the PRM, the only other quantity in the two-state

TABLE III. Electromagnetic quantities from PRM calculations tuned to reproduce the Coulomb excitation data, compared to previous measurements. The $g_K - g_R$ values and the intrinsic matrix elements refer to the hypothetical unperturbed states.

	Tuned PRM	Measured ^a
$\mu(5_{\text{isom}}^-) (\mu_N)$	1.01	0.97(5)
$\mu(1_0^-) (\mu_N)$	0.39	0.3879(15)
$(g_K - g_R)_{K=5}$	-0.22	
$(g_K - g_R)_{K=6}$	-0.0007	
$\langle 6 E2 5 \rangle$ (eb)	+0.016	
$\langle 6 M1 5 \rangle (\mu_N)$	+0.5	

^aFrom Ref. [43].

approximation that directly affects the $M1$ branch intensities is the $\langle K = 6 | M1 | K = 5 \rangle$ intrinsic matrix element. Coulomb excitation calculations using two-state mixing give a positive sign for this intrinsic matrix element, relative to the negative $g_K - g_R$ values for the pure (unperturbed) 5^- and 6^- states, in agreement with the sign predicted by the PRM (Table III).

The matrix elements predicted by the PRM were used to calculate the lifetimes of the states in the $K = 5$ and 6 bands (Fig. 11). Stopping times for the ^{242}Am ions recoiling in the target and its Ni backing are expected to be < 1 ps, so the predicted $\gtrsim 10$ -ps lifetimes of the $I < 15$ levels should result in insignificant Doppler-shift broadening of the observed γ -ray transitions. The excellent fit to the Coulomb excitation data supports this conclusion.

C. Tentative $K^\pi = 5^+, 6^+$ bands

The 30-ns upper limit on the lifetime of the 5^+ state derived from the γ -ray intensity as a function of time and the upper bounds on the unobserved decays from $I > 5$ in the 5^+ band give upper and lower bounds on the $\langle K^\pi = 5^+ | E1 | K^\pi = 5^- \rangle$ matrix elements. The estimated E1 strength that satisfies these bounds is of the order of 10^{-6} W.u. The $\approx 1\%$ normalized yield of the in-band $E2$ transitions and the strength of the $K^\pi = 5^+$ bandhead decay are reproduced by Coulomb excitation

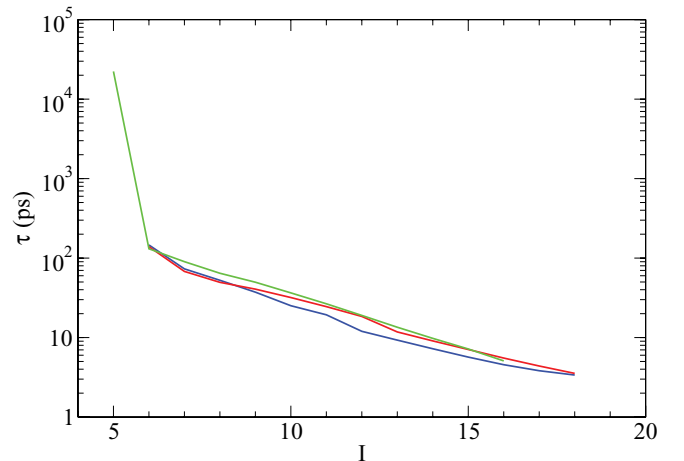


FIG. 11. (Color online) Lifetimes of the 5^- (blue), 6^- (red), and 5^+ (green) states calculated from the final set of matrix elements.

calculations assuming maximum $B(E3; K^\pi = 5^-, 6^- \rightarrow 5^+)$ values of 15 W.u. (Sec. VC). The $E3$ matrix elements were assumed to obey the Alaga rule in the Coulomb excitation calculations.

Assuming that the A and B bands comprise the tentative 6^+ sequence, its population is reproduced by a calculated $E3$ excitation directly from the 5^- band with a strength of ≤ 4 W.u. A two-step $K^\pi = 5^- \xrightarrow{E3} 5^+ \xrightarrow{E2} 6^+$ contribution to the slightly weaker $K^\pi = 6^+$ band population cannot be ruled out. In Coulomb excitation calculations, an $E2$ matrix element of maximum strength ≈ 1 W.u. coupling the 5^+ and 6^+ bands results in a maximum 10% change in the populations of $I > 6$ observed states of the tentative 6^+ band. Because there is no reason to expect $E2$ enhancement in this case (i.e., obviously strong mixing), the $B(E3; K^\pi = 5^- \rightarrow 6^+)$ strength estimated previously is not likely to be affected by a two-step contribution.

D. The unobserved $K^\pi = 2^-, 3^-$ bands

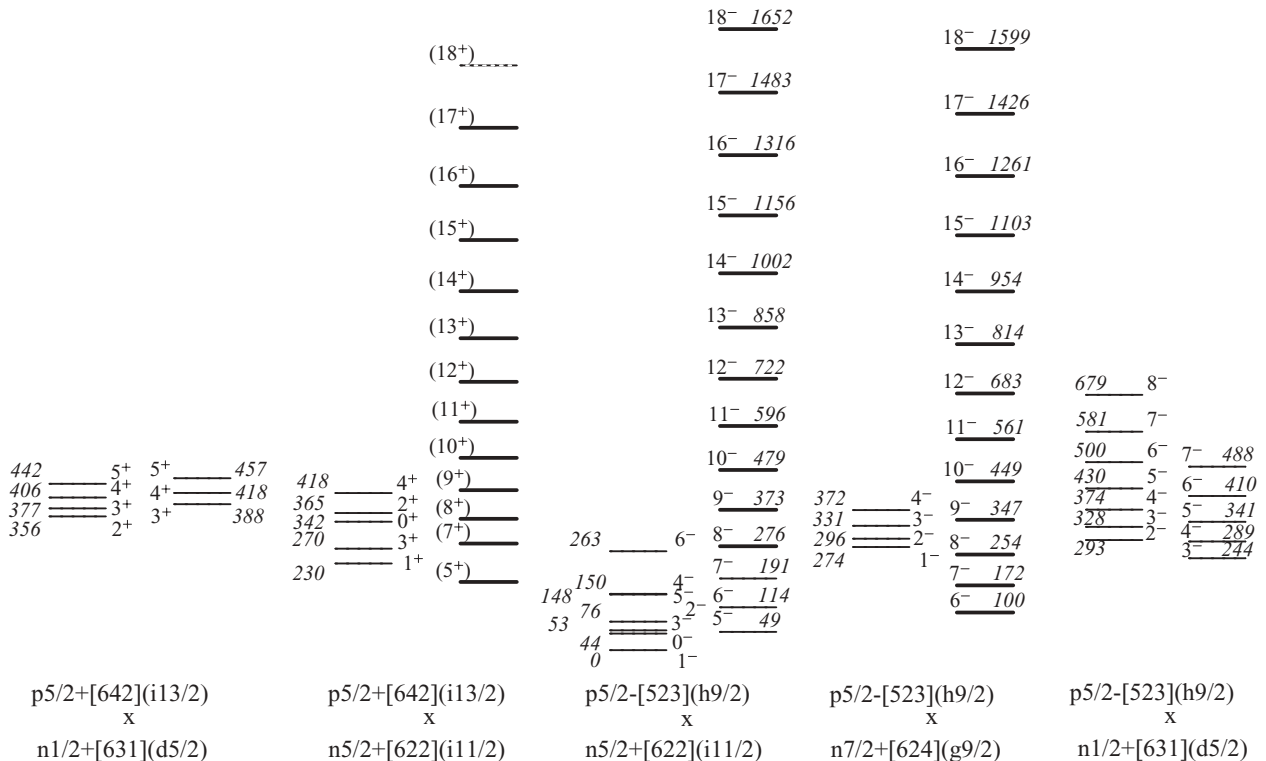
Because $E2$ transitions between the $K^\pi = 5^-$ and the $K^\pi = 3^-$ bands are K allowed and are represented by a one-body EM operator for the previously assigned configurations (Table I), the population of the 3^- band might be expected to be observable in the data. The PRM calculations predict $B(E2)$ values of less than 10^{-2} W.u. coupling the $K^\pi = 2^-, 3^-$ bands to the 5^- sequence. This would result in Coulomb excitation yields below the observable limits in the present data. An upper limit on the in-band $E2$ yields of the $2^-, 3^-$ multiplet can be set at $\sim 1\%$.

The strong peaks from the 5^- and 6^- bands would obscure most of the 3^- bandhead decays, leaving the known 191.7-keV $3_{K=3}^- \rightarrow 3_{K=0}^-$ transition to determine the upper bound on the interband $E2$ strength. The upper limit on this transition is 0.7%, normalized to the $10_5^- \rightarrow 8_5^-$ transition, and the 191.7-keV γ -decay branch is 9% of the total width of the $3_{K=3}^-$ state [15]. Using these limits, Coulomb excitation calculations give an upper limit on the $\langle K^\pi = 3^- | E2 | K^\pi = 5^- \rangle$ strength of ~ 0.5 W.u. The PRM calculations predict a 60%/40% mixing of the $K^\pi = 2^-, 3^-$ bands, which suggests a similar upper bound on the $\langle K^\pi = 2^- | E2 | K^\pi = 5^- \rangle$ matrix element. The multipolarity of the known $I_K^\pi = 2_2^- \rightarrow 3_3^-$ transition is unknown, making it difficult to provide a meaningful upper limit for the 2^- band.

V. DISCUSSION

A. Predicted and observed multiplets

The present experiment provides evidence for Coulomb excited rotational bands built on the two previously unobserved yrast states: the $K^\pi = 6^-$ yrast negative-parity band and the tentatively identified 5^+ yrast positive-parity band, which is coupled to what may be a 6^+ band. The previous $^{243}\text{Am}(d,t)^{242}\text{Am}$ and $^{241}\text{Am}(d,p)^{242}\text{Am}$ experiments [14] selectively populated states in ^{242}Am built on the $\pi_{\frac{5}{2}}^- [523](h_{9/2})$ state (Table I and Fig. 12), the ground-state configuration of both ^{241}Am and ^{243}Am , that is, states reached by the addition or removal of a neutron with respect to the $^{241,243}\text{Am}$ ground states. The ^{242}Am $K^\pi = 5^-$ isomer, the initial state of



the Coulomb excitation in the present experiment, has been established as resulting from the coupling of a proton in the $5/2^-$ [523] Nilsson orbital (of $h_{9/2}$ parentage) to a neutron in the $5/2^+$ [622]($i_{11/2}$) orbital [13,15,44]. The first five multiplets containing the lowest-lying 10 observed bandhead states are given in Table I and Fig. 12. All of these multiplets can be coupled to the 5^- band by a one-particle EM operator, making them among the most likely to be strongly populated by Coulomb excitation from the isomer. Seven of these 10 bandhead states have been identified previously [14,15].

The direct reaction data in Ref. [14] showed two unidentified peaks at 99 and 171 keV, within 1 keV of the states identified in the present work as the 6_6^- and 7_6^- levels. The ratio of the 99- and 171-keV intensities to the 6_5^- and 7_5^- intensities in the direct reaction data is $\approx 13\%$. The ratios of the spectroscopic factors are expected to be 13%–14%, respectively, calculated from the amplitudes of the $i_{11/2}$ and $g_{9/2}$ components in the 45% mixed wave functions of the tuned PRM calculations, in approximate agreement with the measured reaction intensities in Ref. [14].

In previous $^{241}\text{Am}(n,\gamma)$ work [15], no states above $I \approx 5$ were observed, so it is likely that both the $K^\pi = 5^+$ and the $K^\pi = 6^+$ levels would not have been found in the (n,γ) data. The (n,γ) selectivity is also consistent with the lack of previous observation of either the $\pi \frac{5}{2}^+$ [642]($i_{13/2}$) \otimes $\nu \frac{5}{2}^+$ [622]($i_{11/2}$) $K^\pi = 5^+$ state or the $\pi \frac{7}{2}^+$ [633]($i_{13/2}$) \otimes $\nu \frac{5}{2}^+$ [622]($i_{11/2}$) $K^\pi = 6^+$ level, as populating both states requires a one-proton transition from the $^{241,243}\text{Am}$ ground-state proton orbital in addition to the absorption of a neutron.

B. $E2$ strength and enhancement by mixing

The $K^\pi = 6^-$ states are found to be strongly mixed with the $K^\pi = 5^-$ levels. As a result, their Coulomb excitation probabilities are equal, which is a very unusual occurrence owing to a chance degeneracy. The $B(E2)$ values responsible for the observed populations have been reproduced by the tuned PRM calculations. The calculations indicate physically reasonable $B(E2)$ values of ~ 0.02 W.u. coupling the pure states, with an $E2$ enhancement by strong mixing to collective strength, as large as 200 W.u., near the bandheads [Eqs. (4) and (5)]. The matrix elements of the tuned PRM indicate that the initial $5_{\text{isomer}}^- \rightarrow 6_6^-$ step of the Coulomb excitation is most important in reproducing the observed equal populations. In terms of a two-state mixing picture, this is equivalent to the interference effect in cases where the intrinsic quadrupole moments of the states involved are equal [45].

The upper limits on Coulomb excitation of the unobserved $K^\pi = 2^-, 3^-$ bands and the γ -decay transitions of their bandheads were used to set upper bounds on the reduced transition probabilities $B(E2; K^\pi = 5^- \rightarrow K = 3^-)$ and $B(E2; K^\pi = 6^- \rightarrow K = 3^-)$ at ≤ 0.5 W.u. This clearly indicates that there is no enhancement above the typical single-particle transition strength.

C. $E1$ and $E3$ strength

The $B(E1) \sim 10^{-6}$ W.u. strength coupling the $K^\pi = 5^+$ band to the $5^-, 6^-$ sequences is below measured values in the

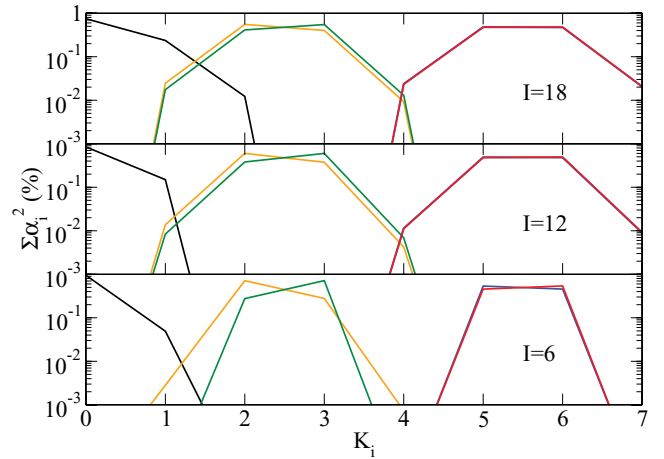


FIG. 13. (Color online) The sum of amplitudes squared $\Sigma\alpha_i^2$ of all components i with the same $K = K_i$ for the wave functions of the 0^- ground state (black), 2_1^- (orange), 3_1^- (green), 5^- isomer (blue), and 6^- (red) rotational bands as predicted by the tuned PRM calculations for $I = 6, 12$, and 18 .

region, for example, 7×10^{-6} W.u. in ^{237}Np and 3×10^{-4} W.u. in ^{239}Np [46]. The excitation of the 5^+ band is consistent with $E3$ matrix elements of a maximum strength estimated at 15 W.u. from the mixed 5^- and 6^- bands. This $E3$ strength is consistent with a one-particle operator changing the $h_{9/2}$ proton in the $K^\pi = 5^-$ component of the mixed 5^- and 6^- wave functions to the $i_{13/2}$ proton of the $K^\pi = 5^+, 0^+$ multiplet. The observed $E3$ strengths in the $A = 240$ region are typically 10–30 W.u. [47]. Recent work on ^{235}U has also found population by $E3$ Coulomb excitation to be competitive with, and in some cases dominant over, population by $E2$ [48] in single-particle transitions. The other member of this multiplet has $K^\pi = 0^+$, and its population would require higher order K mixing, consistent with nonobservation in the present data (Fig. 13).

D. The $K < 2$ bands and higher order K mixing

Significant $\Delta K \geq 2$ mixing would be required to populate the states in the remaining $0^-, 0^+$, and 1^- low-lying bands in ^{242}Am . None of these states was seen in the present data. Coulomb excitation of ^{178}Hf demonstrated sufficient K mixing at $I \approx 12$ in low- K bands to populate high- K levels to at least $\sim 10^{-4}$ strength by up to 14 times K -forbidden transitions. In ^{178}Hf , the yrast band was populated at the 10% level at $I \approx 12$ [49]. In the present data, Coulomb excitation populated the $17\hbar$ state (12 units of spin above the initial state) of the initial (isomer) band at only the 1% level, making an effect at the level observed in ^{178}Hf impossible to detect. Upper limits of the populations by K -forbidden transitions were set at an $\sim 1\%$ normalized yield.

Figure 13 shows the predicted K mixing of the tuned PRM calculations for the isomer, 6^- , and low- K bands. Within this two-particle model space, this mixing would not be expected to have a significant effect on population of the low- K bands. Even two-step excitations to the GSB through the $2^-, 3^-$ bands would be enhanced by only $\approx 0.5\%$ $\Delta K > 1$ mixing at $I = 12$

in the 5^- , 6^- bands, where there is insufficient excitation of the initial-state 5^- band to populate the GSB to observable levels. Calculations using a four-particle basis might predict more significant K mixing in some of the relevant states.

E. Magnetic quantities

The PRM calculation gives magnetic moments of the isomer and the ground state that agree within 4% with previously measured values (Table III). These values are not sensitive to the tuning already described with the exception of the value of $g_s^{\text{eff}}/g_s^{\text{free}}$. The accuracy in reproducing the known magnetic moments promotes confidence in the $g_K - g_R$ value for the 6^- states as well, which is necessary to trust the parameter $\langle K = 6 | M1 | K = 5 \rangle = +0.5 \mu_N$. The fitted interband $M1$ matrix element corresponds to maximum $B(M1; K^\pi = 5^- \rightarrow K^\pi = 6^-)$ values of 10^{-1} W.u. between the pure $K = 5$ and the pure $K = 6$ states. The band mixing enhances the interband $B(M1)$ strength to ≈ 20 W.u. near the 5^- , 6^- bandheads.

F. Rotational mixing

Predictions of the Coriolis interaction are known to exceed measurements by as much as a factor of 2 to 3 in the $A \approx 240$ region, and only *ad hoc* corrections have been proposed [1,39,40]. Studies of rotational mixing in the $150 < A < 180$ [3,50] and $A \approx 240$ regions [1,40] have used fits to the observed level energies and branching ratios which rely on the unperturbed level energies calculated within the Nilsson model. Other analyses have avoided model dependence and used measured $B(E2)$ values and level energies to solve the two- or three-state mixing problem [5,8,51]. These approaches either are restricted to a band crossing or make some assumption regarding the spin dependence of the interaction energy $V(I)$. For example, the $B(E2)$ ratios for interband and intraband $\Delta I = 2$ transitions were used to measure the interaction energy for $27/2 \leq I \leq 35/2$ between $K^\pi = 7/2^-$ and $K^\pi = 23/2^-$ bands in ^{179}W and found to be consistent with the relation $V \sim [I(I+1) - K^2]$ [6,7].

In the present case, the accidental degeneracy between the 5^- and the 6^- bands allowed for precise measurement of the mixing strength $\beta^2 = 45.6_{-1.1}^{+0.3}$ for the $I = 6$ states, which is uniquely determined for the values of the intrinsic frame $\langle 6 | E2 | 5 \rangle$ matrix element and magnetic moments predicted by the PRM (Table III). The mixing strength at low spin is very sensitive to the Coulomb excitation yields. A broader distribution of K values is predicted at high spin by the PRM with $\approx 2\%$ total admixtures of $\Delta K > 1$ at $I > 18$. However, the Coulomb excitation cross section was too weak above $I = 16$ for measurement of $\Delta K > 1$ components in the wave function. To a good approximation, the mixing of the 5^- and 6^- bands predicted by the PRM can be understood as two-state mixing near the $V = \Delta E/2$ limit, as the mixing fraction β^2 is nearly 50%. The effective interaction energy V in the two-state approximation (Fig. 14) was determined from the best-fit mixing strength using both the observed splittings and the perturbed splittings predicted by the PRM. The interaction energy is insensitive to changes in β^2 near the 50% mixing limit, making measurement of V more accurate than estimation of β^2 for the high-spin states. The agreement

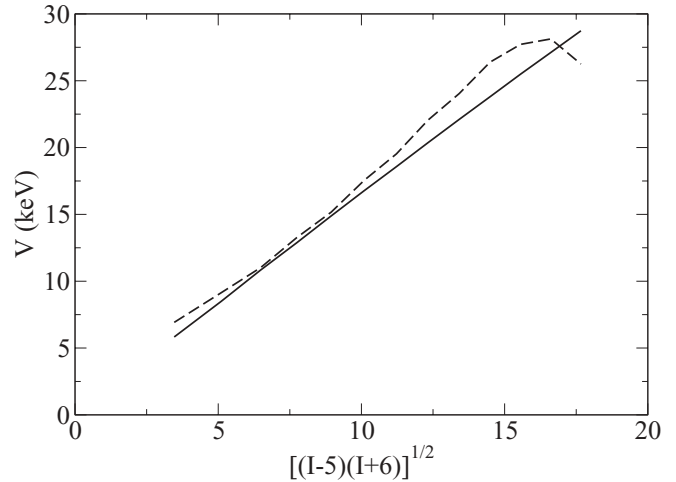


FIG. 14. The mixing matrix element V calculated in the two-state mixing approximation from the mixing predicted by the PRM tuned to reproduce the Coulomb excitation γ -ray yields. The solid line was obtained using the perturbed splittings predicted by the PRM; the dashed line represents the observed splittings.

between these two calculations of V (using the observed splittings and the predicted perturbed splittings of the PRM) confirms that the factor of 2 attenuation of the Coriolis mixing assumed in the PRM calculations is reasonable. (Two-state mixing calculations showed that, using the intrinsic frame matrix elements $\langle 6 | E2 | 5 \rangle$ and $\langle 6 | M1 | 5 \rangle$ as free parameters, an alternative mixing solution with small mixing at the bandheads and larger mixing at higher spin, equally good agreement with the observed γ -ray yields could be obtained, but the resulting fitted value of $\langle 6 | E2 | 5 \rangle$ was inconsistent with the PRM predictions.)

Figure 15 (bottom) demonstrates that the mixing predicted by the PRM can be viewed as two-state mixing: the effect of including all orbitals expected to mix with the $K^\pi = 5^-$ and 6^- configuration is a small shift in the absolute energies (4 keV at $I = 6$, 38 keV at $I = 12$) compared to the predictions where only the Nilsson configurations of the $K^\pi = 5^-$ and 6^- bands are included and the appearance of a crossing of the two bands at $I = 17$, where the calculations predict that predominantly 5^- states become yrast. An up-bend does appear in the alignment (Fig. 16) at $I \approx 17$, but a crossing between the bands cannot be resolved in the data. The excitation energies relative to the mean (Fig. 15, top) demonstrate the repulsive effect of the $\approx 45\%$ mixing and the degeneracy of the unperturbed $K^\pi = 5^-$ and 6^- states in the two-state approximation. Further, these calculations show how strong mixing at all spins would obscure a crossing between the yrast and the nonyrast states by smoothing the excitation energies above and below the crossing and making it difficult to differentiate the two signatures at high spin.

G. Alignments

The alignments in ^{242}Am are given along with those of selected ^{241}Am bands in Fig. 16. Comparing the alignments of the mixed 5^- isomer and 6^- bands to those of the $\pi h_{9/2}$ sequence in ^{241}Am indicates that an additional $\approx 1\hbar$

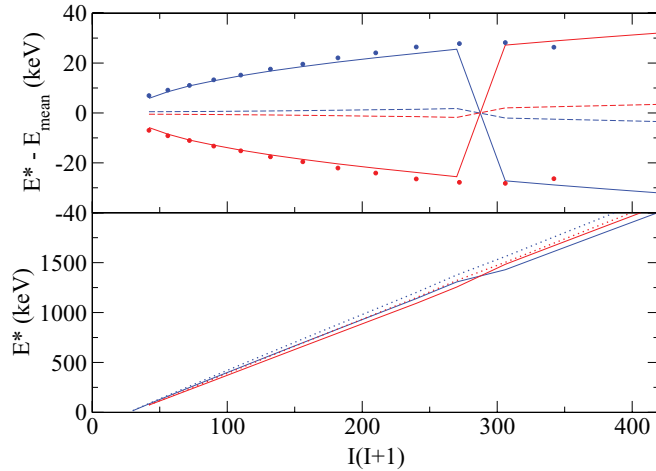


FIG. 15. (Color online) (Top) Excitation energies of the observed 5^- (blue) and 6^- (red) bands relative to the mean energy at each spin for the observed states (symbols) and the tuned PRM predictions (solid lines), compared to the hypothetical unperturbed energies calculated from the observed splittings and the mixing of the PRM calculations (dashed lines). (Bottom) Absolute predicted excitation energies from the PRM including the influence of other orbitals (solid lines), compared to a calculation including only the orbitals that comprise the 5^- and 6^- bands (dotted line). See text for details.

alignment in the former structures comes from the additional neutron component(s). The unperturbed $K^\pi = 5^-$ and 6^- sequences deduced from the tuned PRM using the two-state approximation are nearly degenerate and, therefore, have

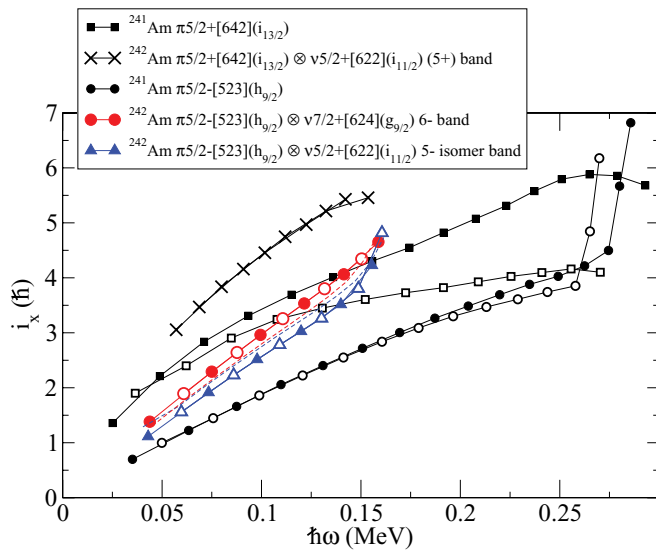


FIG. 16. (Color online) Alignment of the observed bands in ^{242}Am , compared to the alignments of the proton components in ^{241}Am [18]. The Harris parameters $J_0 = 65 \text{ MeV}^{-1} \hbar^2$ and $J_1 = 365 \text{ MeV}^{-3} \hbar^4$ were used in all cases. Dashed lines represent the alignment of the hypothetical unmixed 5^- and 6^- bands obtained from the tuned PRM calculations assuming two-state mixing. Filled symbols indicate the signature whose transitions begin with $I = K + 2$, while open symbols indicate transitions beginning with $I = K + 3$.

virtually identical alignments. This suggests that the $i_{11/2}$ and $g_{9/2}$ neutrons contribute the same amount of alignment, when the repulsive effect of the mixing is removed, at least for $I < 14$, where the Coulomb excitation data provide the sensitivity to tune the PRM.

The first point in the unperturbed 5^- line shows a change in slope, but there is no reason to believe that the unmixed 5^- states should not behave as a good rotor. Because reproduction of the Coulomb excitation γ -ray yield data requires 45% mixing of the $I^\pi = 6^-$ states, this indicates the need for some small residual interaction to maintain smooth rotors in the unperturbed states by introducing a <4 -keV stagger between the even- and the odd-spin unperturbed states.

The tentative $K^\pi = 5^+$ band $[\pi 5/2^+[642](i_{13/2}) \otimes \nu 5/2^+[622](i_{11/2})]$ does not exhibit the splitting between the alignments of the even and odd signatures that is discernible at $\hbar\omega \approx 0.05 \text{ MeV}$ in the $\pi i_{13/2}$ bands of ^{241}Am and ^{237}Np [18]. It should be noted that the spins of these states were chosen so that the alignment is greater than that of the ^{241}Am $i_{13/2}$ structure, as would be expected with the addition of a neutron (Sec. III D).

VI. CONCLUSION

Resolving γ rays from closely spaced excited states in an odd-odd nucleus, in a situation complicated further by the background from a millicurie radioactive target, can pose a seemingly insurmountable experimental challenge. The present work used the selectivity of Coulomb excitation with the sensitivity of the ‘‘Gammasphere plus CHICO’’ detector system to identify 46 new states.

One goal of the experiment was to search for Coulomb excitation of the ground state from the $K^\pi = 5^-$ isomer via K mixing. Neither the known $K^\pi = 0^-$ GSB levels (Fig. 1) nor any candidate states for the extension of the GSB were observed in the γ -ray data. After tuning the PRM to reproduce the observed γ -ray yields of the isomer and 6^- bands, the calculated K mixing predicts insufficient low- K admixtures, within the two-particle model basis, to expect observation of the GSB in the present data.

The 6^- yrast negative-parity bandhead and the tentative $K^\pi = 5^+$ yrast bandhead were found to lie within 25 keV of their predicted energies [15]. Including these states, 9 of the 10 lowest predicted $\pi \otimes \nu$ multiplets in ^{242}Am have been identified from this and previous work. States with spin greater than about $5\hbar$ were not populated in previous (n, γ) reactions, while direct reaction studies favored levels built on the $h_{9/2}$ proton orbital, preventing previous identification of the $K^\pi = 5^+$ band [14,15]. A band feeding the 5^+ band was suggested to be the predicted $K^\pi = 6^+$ sequence.

An unexpected outcome of the present study was the identification of two strongly mixed $K^\pi = 5^-$ and 6^- bands. The 5^- band of the initial isomeric state and the 6^- band were populated equally by Coulomb excitation, a very unlikely occurrence even for strongly coupled collective excitations. The tuned PRM calculations support the conclusion that there is strong mixing of good- K states by a first-order ($\Delta K = 1$) interaction (in the two-state mixing approximation). Applicability of the two-state approximation is supported by

the PRM calculations. This accidental degeneracy allowed for precise measurement of the interaction energy between the 5^- and the 6^- bands. A slightly broader distribution of K values is predicted at high spin by the PRM with $\approx 2\%$ total admixtures of $\Delta K > 1$ at $I > 18$, beyond the reach of this measurement. The Coulomb excitation calculations using the results of the PRM indicate that the assumption of 50% attenuation of Coriolis mixing typical in the actinides is reasonable in the present case. The tuned PRM calculations suggest that the mixing between the 5^- and the 6^- bands is $\approx 45\%$ for $6 \leq I \leq 18$, very near the strong-mixing limit. This level of mixing reproduces the ratio of the cross sections of the two states suspected to be $I_K^\pi = 6_6^-, 7_6^-$, relative to the cross sections of the $I_K^\pi = 6_5^-, 7_5^-$ states in the previous $^{243}\text{Am}(d,t)^{242}\text{Am}$ reaction data.

While upper limits on the γ -ray intensities of the unobserved $K^\pi = 2^-, 3^-$ sequences provide upper bounds of ≤ 0.5 W.u. on the $B(E2)$ values coupling the mixed $5^-, 6^-$ bands to the $K^\pi = 2^-, 3^-$ bands and the $E2$ strength coupling the pure $K^\pi = 5^-$ components to the $K^\pi = 6^-$ components was ≈ 0.02 W.u. (assuming two-state mixing), strong $K = 5, 6$ mixing resulted in enhancements to collective strength as large as 200 W.u. Higher ΔK transitions were not observable, making higher order K mixing unmeasurable. The $B(M1)$ strength coupling the $5^-, 6^-$ bands was also enhanced by the K mixing from 10^{-1} W.u. for the pure $K = 5, 6$ unperturbed levels to ≈ 20 W.u. for the observed states.

The deduced $E1$ and $E3$ strengths coupling the tentative $K^\pi = 5^+$ band to the 5^- and 6^- bands were of the order of 10^{-6} and 15 W.u., respectively. The $E3$ coupling of the tentative $K^\pi = 6^+$ sequence to the negative-parity bands was estimated to be ~ 1 W.u. Both the $B(E1)$ and the $B(E3)$ values are similar to previous measurements in the $A \approx 240$ region,

where $E3$ Coulomb excitation was found to be competitive with $E2$ excitation.

A large change in alignment of the $\pi h_{9/2}$ orbital in ^{241}Am occurs at a frequency of $\hbar\omega > 0.25$ MeV. Coulomb excitation with the low- Z ^{40}Ar nucleus was unable to reach beyond $\hbar\omega = 0.15$ MeV, but an apparent onset of alignment in the predominantly $\pi h_{9/2} \otimes \nu i_{11/2}$ and $\pi h_{9/2} \otimes \nu g_{9/2}$ states of the 5^- isomer band was observed at this frequency. Comparisons were made between the proton orbitals in neighboring ^{241}Am and the presently observed states that have an additional neutron.

ACKNOWLEDGMENTS

The authors wish to thank A. O. Macchiavelli of Lawrence Berkeley National Laboratory for advice and assistance with the detector electronics. We thank R. W. Hoff of Lawrence Livermore National Laboratory (LLNL) for correctly suggesting the identity of the 6^- band and D. C. Radford for correctly identifying the doublets in the $K^\pi = (5^+)$ band to be distinct from the 5^- band transitions. This work was supported by the Air Force Office of Scientific Research under Contract Nos. FA9550-05-1-0022 (Rochester) and FA9550-05-1-0486 (Youngstown and S.A.K.), the Swedish Science Research Council (I.R.), DTRA Contract No. HDTRA1-08-1-0014 (Youngstown and S.A.K.), the National Science Foundation (Rochester), and the US Department of Energy, Office of Nuclear Physics, under Contract No. DE-AC02-06CH11357 (ANL). The LLNL work was performed under the auspices of the US Department of Energy in part by the University of California under Contract No. W-7405-ENG-48 and in part by the LLNL, operated by Lawrence Livermore National Security, LLC, under Contract No. DE-AC52-07NA27344.

-
- [1] F. S. Stephens, M. D. Holtz, R. M. Diamond, and J. O. Newton, *Nucl. Phys. A* **115**, 129 (1968).
- [2] G. D. Dracoulis *et al.*, *Phys. Rev. Lett.* **97**, 122501 (2006).
- [3] O. W. B. Schult *et al.*, *Phys. Rev.* **154**, 1146 (1967).
- [4] C. Y. Wu, D. Cline, M. W. Simon, G. A. David, R. Teng, A. O. Macchiavelli, and K. Vetter, *Phys. Rev. C* **64**, 064317 (2001).
- [5] P. M. Walker, *J. Phys. G* **34**, 123 (2007).
- [6] P. M. Walker, G. D. Dracoulis, A. P. Byrne, B. Fabricius, T. Kibedi, and A. E. Stuchbery, *Phys. Rev. Lett.* **67**, 433 (1991).
- [7] P. M. Walker, G. D. Dracoulis, A. P. Byrne, B. Fabricius, T. Kibedi, A. E. Stuchbery, and N. Rowley, *Nucl. Phys. A* **568**, 397 (1994).
- [8] P. M. Walker, K. C. Yeung, G. D. Dracoulis, P. H. Regan, G. J. Lane, P. M. Davidson, and A. E. Stuchbery, *Phys. Lett. B* **309**, 17 (1993).
- [9] A. A. Zadernovsky and J. J. Carroll, *Hyperfine Interact.* **143**, 153 (2002).
- [10] J. J. Carroll, S. A. Karamian, L. A. Rivlin, and A. A. Zadernovsky, *Hyperfine Interact.* **135**, 3 (2001).
- [11] J. J. Carroll, *Laser Phys. Lett.* **1**, 275 (2004).
- [12] A. Pálffy, J. Evers, and C. H. Keitel, *Phys. Rev. Lett.* **99**, 172502 (2007).
- [13] F. Asaro, I. Perlman, J. O. Rasmussen, and S. G. Thompson, *Phys. Rev.* **120**, 934 (1960).
- [14] T. Grottdal, L. Guldberg, K. Nybø, and T. F. Thorsteinsen, *Phys. Scripta* **14**, 263 (1976).
- [15] J.-L. Salicio, S. Drissi, M. Gasser, J. Kern, H. G. Börner, G. G. Colvin, K. Schreckenbach, R. W. Hoff, and R. W. Lougheed, *Phys. Rev. C* **37**, 2371 (1988).
- [16] M. W. Simon, D. Cline, C. Y. Wu, R. W. Gray, R. Teng, and C. Long, *Nucl. Instrum. Methods A* **452**, 205 (2000).
- [17] I.-Y. Lee, *Nucl. Phys. A* **520**, 641c (1990).
- [18] K. Abu Saleem *et al.*, *Phys. Rev. C* **70**, 024310 (2004).
- [19] National Nuclear Data Center (2005) Online databases; [<http://www.nndc.bnl.gov>].
- [20] R. B. Firestone, *Table of Isotopes*, 8th ed. (Wiley & Sons, New York, 1996), vol. 2.
- [21] T. Lauritsen *et al.*, *Phys. Rev. C* **75**, 064309 (2007).
- [22] Gammasphere (1998) Online documentation; [<http://www.phy.anl.gov/gammasphere/doc/efficiency>].
- [23] R. Brun, F. Bruyant, M. Maire, A. C. McPherson, and P. Zanarini, *GEANT3 User's Guide, DD/EE/84-1* (CERN, Geneva, 1987).
- [24] M. W. Simon, Ph.D. dissertation, University of Rochester, 1999.
- [25] R. Marrus and J. Winocur, *Phys. Rev.* **124**, 1904 (1961).

- [26] J. Kantele and O. Tannila, *Nucl. Data A* **4**, 359 (1968).
- [27] T. Kibedi, T. W. Burrows, M. B. Trzhaskovskaya, P. M. Davidson, and J. C. W. Nestor, *Nucl. Instrum. Methods A* **589**, 202 (2008).
- [28] K. Abu Saleem, Ph.D. dissertation, Illinois Institute of Technology, 2002.
- [29] A. B. Hayes *et al.*, *Las. Phys.* **17**, 745 (2007).
- [30] I. Ragnarsson and P. B. Semmes, *Hyperfine Interact.* **43**, 423 (1988).
- [31] S. E. Larsson, G. Leander, and I. Ragnarsson, *Nucl. Phys. A* **307**, 189 (1978).
- [32] T. Czosnyka, D. Cline, and C. Y. Wu, *Bull. Am. Phys. Soc.* **28**, 745 (1983).
- [33] GOSIA Web site (2008) [<http://www.pas.rochester.edu/~cline/Gosia>].
- [34] P. Rozmej, K. Boning, and A. Sobiczewski, in *Proceedings of the XXIV International Winter Meeting on Nuclear Physics, Bormio, Italy*, edited by I. Iori (Ric. Sci. Educ. Permanente, Bormio, 1986), p. 567.
- [35] C.-D. Herrmann, B. Prillwitz, U. Dammrich, K. Freitag, P. Herzog, D. Mayer, K. Schlosser, and I. Ragnarsson, *Nucl. Phys. A* **493**, 83 (1989).
- [36] P. Moller and J. R. Nix, *At. Data Nucl. Data Tables* **26**, 165 (1981).
- [37] S. Raman, C. W. N. Jr., and P. Tikkanen, *At. Data Nucl. Data Tables* **78**, 1 (2001).
- [38] S. G. Nilsson, C. F. Tsang, A. Sobiczewski, Z. Szymanski, S. Wycech, C. Gustafson, I.-L. Lamm, P. Moller, and B. Nilsson, *Nucl. Phys. A* **131**, 1 (1969).
- [39] A. Bohr and B. R. Mottelson, *Nuclear Structure*, vol. 2 (Benjamin/Cummings, Reading, MA, 1975).
- [40] D. Ward *et al.* (unpublished).
- [41] R. R. Chasman, I. Ahmad, A. M. Friedman, and J. R. Erskine, *Rev. Mod. Phys.* **49**, 833 (1977).
- [42] K. Alder and A. Winther, *Electromagnetic Excitation* (American Elsevier, New York, 1975).
- [43] Y. A. Akovali, *Nucl. Data Sheets* **96**, 177 (2002).
- [44] R. W. Hoff, J. Kern, R. Piepenbring, and J. P. Boisson, in *Proceedings of Conference on Capture Gamma-Ray Spectroscopy and Related Topics*, edited by S. Raman (Am. Inst. Phys., New York, 1985).
- [45] R. F. Casten, *Nuclear Structure from a Simple Perspective* (Oxford University Press, New York, 2000).
- [46] I. Ahmad and P. A. Butler, *Annu. Rev. Nucl. Part. Sci.* **43**, 71 (1993).
- [47] R. H. Spear, *At. Data Nucl. Data Tables* **42**, 55 (1989).
- [48] D. Ward *et al.*, *AIP Conf. Proc.* **764**, 263 (2005).
- [49] A. B. Hayes *et al.*, *Phys. Rev. C* **75**, 034308 (2007).
- [50] A. K. Kerman, *Mat. Fys. Medd. Dan. Vid. Selsk.* **30** (1956).
- [51] T. Shizuma, S. Mitarai, G. Sletten, R. A. Bark, N. L. Gjørup, H. J. Jensen, J. Wrzesinski, and M. Piiparinen, *Nucl. Phys. A* **593**, 247 (1995).